Numerical Investigation of the Effect of Vertical Load on the Lateral Response of Piles

S. Karthigeyan[1]; V. V. G. S. T. Ramakrishna[2]; and K. Rajagopal[3]

Abstract: The laboratory and field test data on the response of piles under the combined action of vertical and lateral loads is rather limited. The current practice for design of piles is to consider the vertical and lateral loads independent of each other. This paper presents some results from three-dimensional finite-element analyses that show the significant influence of vertical loads on a pile's lateral response. The analyses were performed in both homogeneous clayey soils and homogeneous sandy soils. The results have shown that the influence of vertical loads on the lateral response of piles is to significantly increase the capacity in sandy soils and marginally decrease the capacity in clayey soils. In general, it was found that the effect of vertical loads in sandy soils is significant even for long piles, which are as long as 30 times the pile width, while in the case of clayey soils, the effect is not significant for piles beyond a length of 15 times the width of the pile. The design bending moments in the laterally loaded piles were also found to be dependent on the level of vertical load on the piles.

DOI: 10.1061/(ASCE)1090-0241(2007)133:5(512)

CE Database subject headings: Piles; Lateral loads; Finite element method; Combined loads; Numerical models.

Introduction

Pile foundations are extensively used to support various structures built on loose/soft soils, where shallow foundations would undergo excessive settlements or shear failure. These piles are used to support vertical loads, lateral loads, or a combination of vertical and lateral loads. However, in view of the complexity involved in analyzing the piles under combined loading, the current practice is to analyze the piles independently for vertical loads to determine their bearing capacity and settlement and for the lateral load to determine their flexural behavior.

The methods of analysis commonly used in predicting the behavior of piles and pile groups under pure axial loads could be categorized into (1) subgrade reaction method (Coyle and Reese 1966; Kraft et al. 1981; Zhu and Chang 2002); (2) elastic continuum approaches (Poulos 1968; Xu and Poulos 2000); and (3) finite-element methods (Desai 1974; Trochanis et al. 1991; Wang and Sitar 2004). Similarly, the methods to study the behavior of piles and pile groups under pure lateral loads could be categorized into (1) limit state method (Broms 1964); (2) subgrade reaction method (Matlock and Reese 1960); (3) elastic continuum approach (Poulos 1971; Banerjee and Davis 1978); (4) *p-y* method (Reese et al. 1974); and (5) finite-element methods (Muqtadir and Desai 1986; Brown and Shie 1991; Trochanis et al. 1991; Kimura et al. 1995; Yang and Jeremic 2002; Yang and Jeremic 2005).

Studying the interaction effects on piles under combined loads would no doubt call for a systematic and sophisticated analysis. The literature available in this field is sparse. The limited information on this topic based on analytical investigations (Davisson and Robinson 1965; Ramasamy 1974; Goryunov 1975) reveals that for a given lateral load, the lateral deflection increases with the combination of vertical loads. However, experimental (Pise 1975; Sarochan and Bykov 1976; Jain et al. 1987) and field investigations (McNulty 1956; Bartolomey 1977; Zhukov and Balov 1978) suggest a decrease in lateral deflection with the combination of vertical loads. Anagnostopoulos and Georgiadis (1993) attempted to explain this phenomenon through an experimental model supported by two-dimensional (2D) finite-element analysis and reported that the modified status of soil stresses and local plastic volume changes in the soil continuum under combined vertical and lateral loads cannot in general be accounted for by the conventional subgrade reaction, elastic half space, and other 2D approaches. Thus a nonlinear three-dimensional (3D) finite-element analysis would be the most appropriate approach. Trochanis et al. (1991) attempted to study the axial response of piles with the combination of lateral loads through 3D finite-element analysis. Since the piles are not often adequately designed to resist lateral loads, the response of piles under lateral load in the presence of vertical loads is more critical and interesting for the design engineers. Besides, the influence of the pile slenderness ratio (L/B) is also an important parameter to be considered in pile design. In view of this, the present paper focuses on the study of piles subjected to pure lateral loads and combined vertical and lateral loads through 3D finite-element analyses. The details of the numerical model, the validation of the developed model against some field cases, and results from parametric studies are discussed in the paper.

[1]Scientist, Central Building Research Institute, Roorkee, 247 667 India. E-mail: mahamaha2001@yahoo.com

[2]Scientist, Central Building Research Institute, Roorkee, 247 667 India. E-mail: vvgst@yahoo.com

[3]Professor, Dept. of Civil Engineering, Indian Institute of Technology, Madras, Chennai, 600 036 India. E-mail: gopalkr@iitm.ac.in

Note. Discussion open until October 1, 2007. Separate discussions must be submitted for individual papers. To extend the closing date by one month, a written request must be filed with the ASCE Managing Editor. The manuscript for this paper was submitted for review and possible publication on January 27, 2006; approved on November 9, 2006. This paper is part of the ***Journal of Geotechnical and Geoenvironmental Engineering***, Vol. 133, No. 5, May 1, 2007. ©ASCE, ISSN 1090-0241/2007/5-512–521/$25.00.

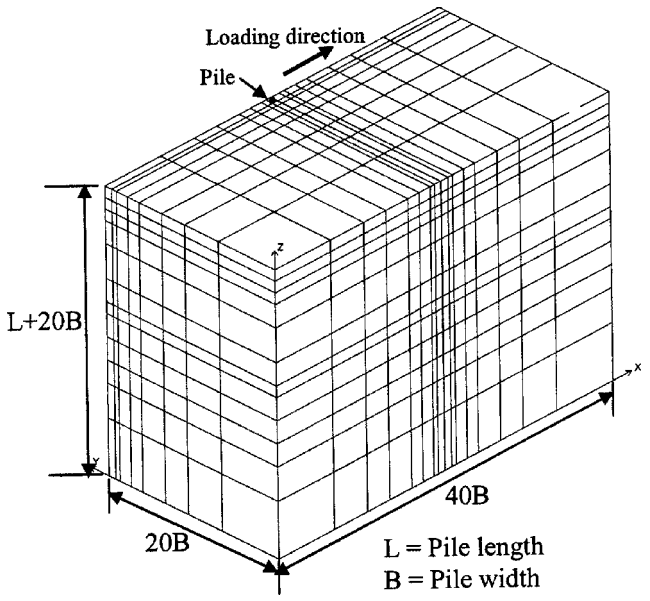

Fig. 1. Typical mesh used for 3D finite-element analyses

Numerical Model

All finite-element analyses in this investigation were performed using the 3D finite-element program, GEOFEM3D, developed by the writers. The program is supported by a preprocessor to develop 3D meshes consisting of bar and beam type prismatic elements, 8-node or 20-node isoparametric brick elements, 8- or 16-node zero thickness type interface elements as well as a post-processing tool that is capable of plotting the original mesh, deformed mesh, displacement vectors, extracting nodal displacements, and element stresses along a line/selected plane, etc.

Mesh Details

Fig. 1 shows a schematic 3D finite-element mesh for analysis of pile-soil interaction. Based on the symmetry, only half the pile section in the direction of lateral load is analyzed (in Fig. 1, lateral load is applied along the x-axis). 20-node brick elements are used to mesh the pile and the soil continuum. The interface between the pile and the soil has been modeled using 16-node joint elements of zero thickness. All numerical computations of isoparametric elements were performed using reduced numerical integration. The mesh dimensions, number of nodes, and elements in the mesh were decided after performing a number of initial trial analyses with several meshes of increasing refinement until the results (displacements and stresses around the pile) did not change significantly with further refinement. The aspect ratios of elements used in the mesh ranged from 0.5 near the pile surface to nearly 5 at the boundaries. The distances to lateral rigid boundaries in the finite-element analyses are shown in Fig. 1. All the nodes on the lateral boundaries were restrained from moving in the normal direction to the respective surfaces representing rigid, smooth lateral boundaries. All the nodes on the bottom surface were restrained in all three directions representing the rough, rigid bottom surface. Typically, the meshes consisted of approximately 8,300 nodes, 1,440 20-node brick elements, and 52 16-node interface elements.

Pile-Soil Details

The pile was treated as a linear elastic material. The Von Mises constitutive model with associated flow rule for clayey soils (Yang and Jeremic 2002; Wang and Sitar 2004) and the Drucker-Prager constitutive model with nonassociated flow rule for sandy soils (Trochanis et al. 1991; Yang and Jeremic 2005) were used to predict the stress-strain behavior. These models have been used because they are able to define the failure criterion by using simple physical properties such as cohesion (c) and friction angle (ϕ). The failure criterion for the Drucker-Prager model used for sandy soils has the form $F=\alpha J_1+\sqrt{J_{2d}}-k$, in which J_1=first invariant of the stress tensor, J_{2d}=second invariant of the deviatoric stress tensor, and α, k are material constants expressed in terms of the well-known shear strength parameters of soil with respect to c and ϕ. For clayey soils, α is zero and this equation reduces to $F=\sqrt{J_{2d}}-k$ representing the Von Mises criterion.

During the plastic flow, the elastic constitutive matrix was first formed based on the current tangent modulus and Poisson's ratio of the material. Then a correction was applied to obtain the elastic-plastic constitutive matrix. The stresses were corrected back to the yield surface along the flow direction (normal to the potential surface defined by the dilation angle ψ) as described by Nayak and Zienkiewicz (1972).

Analysis Scheme

The finite-element analyses were performed in two stages. In the first stage, the in situ stresses were initialized in the soil by performing a dummy analysis using a modified Poisson's ratio (μ') expressed in terms of the at rest earth pressure coefficient K_o as $\mu'=K_o/(1+K_o)$. The value of K_o itself was obtained as $K_o=1-\sin\phi$. During this stage of analysis, both the pile and the soil elements were assigned the same material properties corresponding to the soil (Young's modulus, Poisson's ratio, and unit weight) so as not to generate any extraneous shear stresses. At the

Table 1. Properties of Pile and Soil

	Soil details	
Pile details	Clayey soils	Sandy soils
Size: 1200×1200 mm square	Undrained cohesion c_u=100 kPa	ϕ=36°
Length: 10 m	Friction angle (ϕ)=0°	ψ=12°
Type of pile: Concrete	Dilation angle (ψ)=0°	c_u=0.0
Grade of concrete: M25	Young's modulus (E_s)=40 MPa	E_s=50 MPa
Young's modulus E_p: 25,000 MPa	Poisson's ratio (μ_s)=0.40	μ_s=0.30
Unit weight (γ_p): 24 kN/m^3	Unit weight (γ_s)=18 kN/m^3	γ_s=20 kN/m^3
Poisson's ratio μ_p: 0.15	Earth pressure (K_o)=0.60	K_o=0.41

end of this stage of analysis, all the deformations and strains are set to zero to define the datum level for further analysis.

During the second stage of analysis, the actual properties of the soil and the pile elements were assigned to them. The set of pile-soil properties considered in the analyses are summarized in Table 1.

The shear strength of the interfaces was defined with zero cohesive strength and 2/3 of the friction angle for sandy soils. In the case of clayey soils, the interfaces were assumed to have zero frictional strength and 2/3 of the cohesive strength of the surrounding soil. The interface strength values depend very much on the type of pile material (wood, steel, or concrete) and method of installation (driven or bored). The interface strength properties selected for the analyses fall within the range of properties recommended for estimating the skin friction capacity of piles (Bowles 1988). The normal stiffness and shear stiffness of the interface elements were initially set to 10^6 kN/m^2/m. These values were decided after performing several analyses with different interface stiffness values. After the shear failure of the interface, the shear stiffness is set to 0.1% of the initial value to permit the relative slip between different materials. The normal stiffness of the interface is set to 0.1% of the initial value when tensile normal stresses develop to permit the separation between the pile and the soil.

The external loads were applied in small increments in several load steps with several iterations to satisfy the system's equilibrium. The iterations were continued at each load step until the norms of out-of-balance force and the incremental displacements were less than 0.5% or until 50 iterations were completed. The analyses were performed using a partial Newton-Raphson scheme by updating the stiffness matrix only at the first iteration of each load step.

Validation of the Numerical Model

The validity of the numerical model employed in the program was verified by predicting the pile load test data from two different published cases, one with respect to a short rigid pile under combined vertical and lateral loads and another for a long flexible pile under pure lateral load. The details of these two cases are presented in the following sub-sections.

Case Study 1 (Kimura et al. 1995)

Kimura et al. (1995) reported the response of 30.4 m long, 1.2 m diameter cast-in-place reinforced concrete piles under lateral loads installed at Kishiwada Great Bridge on the Hanshin Expressway in Osaka. The subsoil at the site consists of an upper 10 m of backfilled sandy gravel and a lower layer made up of mixed alternate layers of clay and sand. The soil and interface properties used in the current analysis are the same as those reported by Kimura et al. (1995). Using symmetry, only half of the pile was considered in the analysis. The same sequence of load application followed in the field test was used in the present finite-element analysis. The comparison between the present predictions and the measured results reported by Kimura et al. (1995) is shown in Fig. 2. There is an excellent comparison between the present numerical results and the field test data up to a lateral displacement equal to about 10% of the pile diameter. Even at larger displacements, the difference between the predicted and the measured results is less than 7%, which is within reasonable limit in view of the variability of soil properties.

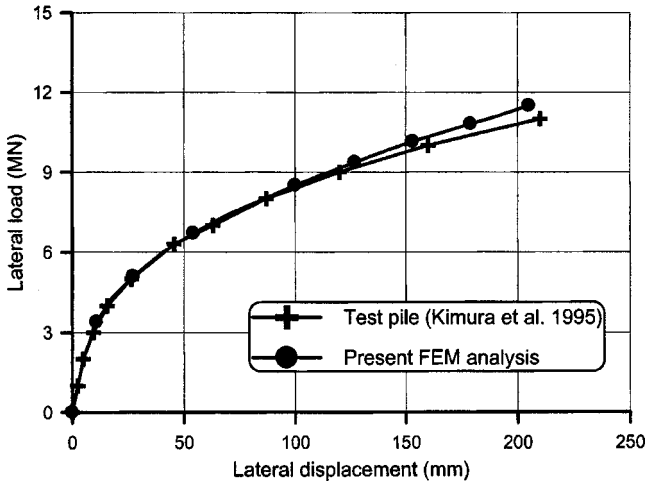

Fig. 2. Comparison of FEM predicted results with test data of Kimura et al. (1995)

Case Study 2 (Anagnostopoulos and Georgiadis 1993)

This case study pertains to laboratory model tests on aluminium closed-ended piles of 19 mm outside diameter and 1.5 mm wall thickness, jacked 500 mm into a prepared soft clay bed (w_L=42%, w_p=24%, and c_u=28 kN/m^2) (Anagnostopoulos and Georgiadis 1993). The laboratory tests were performed on single pile under both vertical and lateral loads applied to the pile head at ground elevation through dead weights. The combined loads were applied in two stages: in the first stage a vertical load of 160 N was applied and in the second stage the lateral load of 130 N was applied incrementally. The Young's modulus (E_s) of the soil was taken as 7,500 kPa using the relation $E_s \approx 250-400 \times c_u$ (Poulos and Davis 1980). The Poisson's ratio of the clayey soil was taken as 0.49, assuming an undrained response during the load test. The soil was idealized as a Von Mises material. The pile was modeled as a solid pile with an equivalent modulus to match the flexural rigidity of the hollow test pile. The sequence of the load application used in the current finite-element analysis is the same as that followed during the laboratory tests. The comparison between the test data and the predicted results of piles under pure vertical load and combined vertical and lateral loads are shown in Figs. 3(a and b). It could be observed that the comparison is very good both at small and larger load levels. The percentage difference is less than 10% at all load levels for both the vertical and lateral responses of the piles.

The finite-element prediction in both the cases matched reasonably well with the test data. Hence, it could be concluded that the numerical scheme adopted in the present investigation is capable of modeling the pile-soil interaction under pure vertical load, lateral load, and a combination of vertical and lateral loads.

Parametric Studies

A series of 3D finite-element analyses were performed on a single free-headed pile in both homogeneous clayey and sandy soils separately. The dimensions of the pile and the soil properties considered in these analyses are reported in Table 1. The response of the piles under pure lateral load was analyzed initially. For studying the response of piles under combined loads, the influence of vertical loads equal to 0.2 V_{ult}, 0.4 V_{ult}, 0.6 V_{ult}, and 0.8 V_{ult} were considered (where V_{ult}=ultimate vertical load capacity, evaluated a priori by a separate numerical analysis). The ultimate vertical

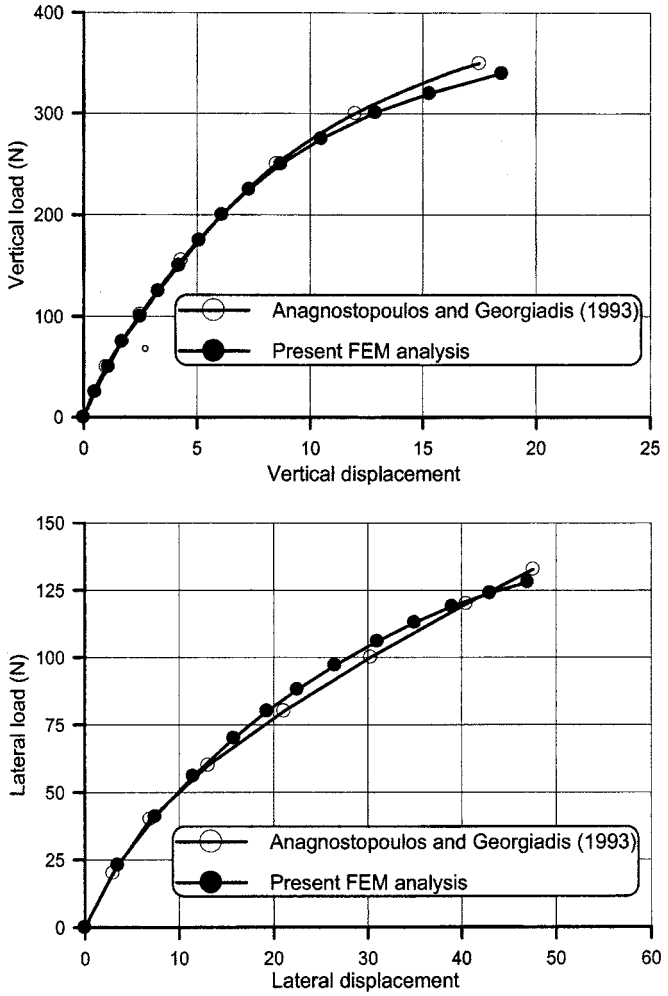

Fig. 3. Comparison of FEM predicted vertical and lateral response of pile with experimental test data of Anagnostopoulos and Georgiadis (1993): (a) vertical response of pile; (b) lateral response of pile

load capacities were estimated as 4,000 kN and 1,920 kN (corresponding to the point with maximum curvature on the vertical load-settlement response) for clayey soil and sandy soil, respectively, through analysis of a single pile subjected to a pure vertical load.

The combined loads are applied in two stages. In the first stage, vertical loads were applied and then in the second stage, lateral loads were applied while the vertical load was kept constant. This type of loading is similar to that in field situations such as pile jetties, transmission line towers, and overhead water tanks, etc. Here, the piles are first subjected to vertical loading from the weight of the deck or superstructure. The lateral loading may be caused by wind, wave loading, ship impact, etc. while the piles are subjected to vertical loads. The analysis in the lateral direction was performed using displacement control (rather than load control) so that the lateral loads developed at various lateral displacement levels could be evaluated as a percentage of the pile size. The reaction forces developed at the nodes were used to calculate the lateral load corresponding to the applied lateral displacements. The numerical results under pure lateral loads and combined lateral and vertical loads on piles are presented and discussed separately for sandy soils and clayey soils in the following sections.

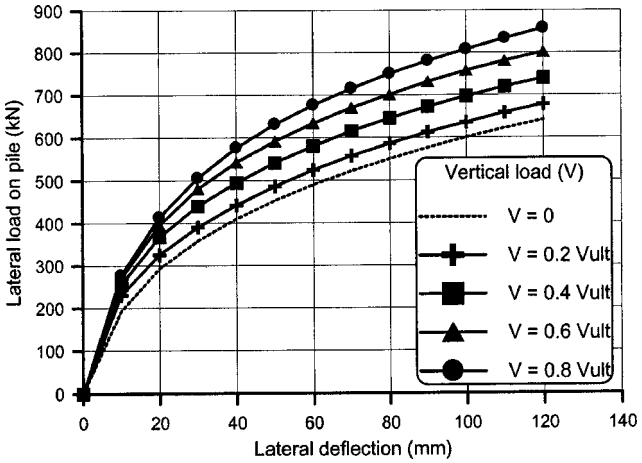

Fig. 4. Lateral load-deflection curves of piles in sand

A few analyses were also performed with different slenderness ratios (L/B) of piles to study the ratio's influence on piles with combined loading.

Results and Discussions

Influence in Homogeneous Sandy Soils

Fig. 4 shows the influence of vertical load on the lateral response of piles in sandy soils. From the data presented, it is noted that the lateral load capacity increases considerably under increased vertical load levels. The loads shown in the figure correspond to the symmetric half of the pile section. It can be noted that the lateral load capacities increase significantly, in the order of 7 to 40% at deflection levels of 0.05B and of the order of 6 to 33% at deflection levels of 0.1B.

The reason for increase in the lateral capacity under the action of vertical load has been examined through variations in lateral deflection and soil stresses along the depth of the piles in Figs. 5–8. Fig. 5 presents the variation in lateral deflection along the pile depth at a reaction load level of 641 kN (load developed at a deflection of 0.1B under pure lateral loading). This figure shows

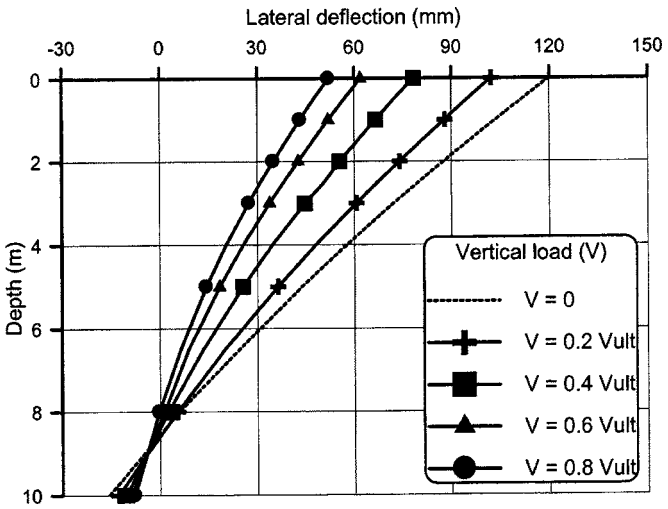

Fig. 5. Variation of lateral deflection along depth of piles in sand

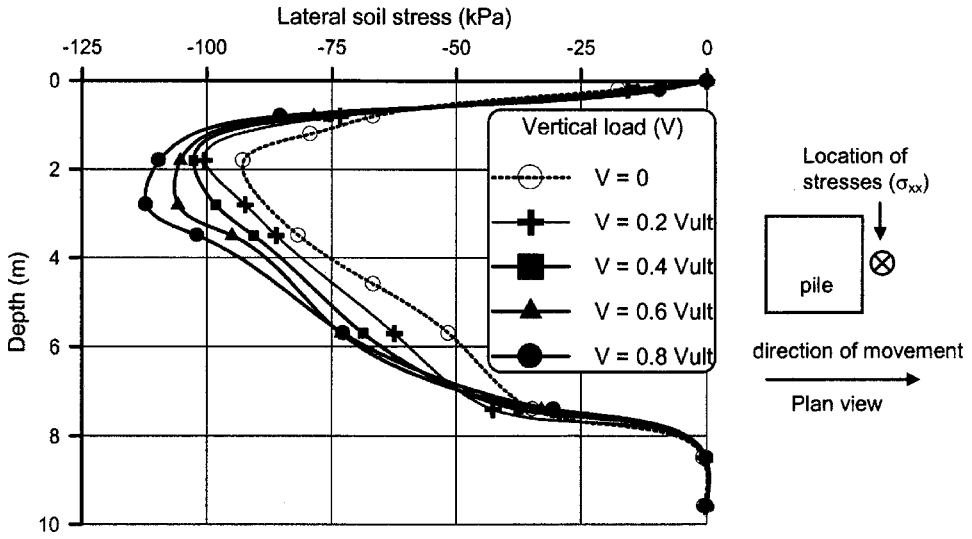

Fig. 6. Variation of lateral soil stresses (σ_{xx}) along depth of piles in sand

that the lateral deflections along the pile depth reduced considerably with increasing vertical load levels. Typical lateral soil stresses (σ_{xx}) in front of the pile and shear stresses (σ_{xy}) on the frictional face of the pile at a lateral deflection of 0.1B are substantially higher at larger vertical load levels as illustrated in Figs. 6 and 7. This increase can be directly attributed to the increase in confining stress with increasing vertical loads at different depths caused by the action of vertical load on the pile. This increased confining stress allows for the development of larger lateral and shear stresses along the pile's frictional face as a result of the increased shear strength of the soil. The increase in lateral soil stresses is further examined through the contours of lateral stresses (σ_{xx}) around the pile under pure lateral load and in the presence of a vertical load of $0.8V_{ult}$ in Figs. 8(a and b). These contours are plotted for a lateral deflection equal to 0.1B and at a depth of 2.8 m from the ground surface (the depth where maximum lateral soil stresses occur, Fig. 6). Similarly, the increase in shear stresses (σ_{xy}) over the pile's frictional face is also examined through the contours of shear stresses around the pile under pure lateral load and in the presence of a vertical load of $0.8V_{ult}$ in Figs. 8(c and d). These contours are plotted at a lateral deflection of 0.1B and at a depth of 2.8 m from the ground surface (i.e., the depth at which maximum shear stress occurs, Fig. 7). It is clear that the lateral soil stress and the mobilized shear stresses of soil around the pile are higher in the presence of vertical load as compared to the pure lateral load case.

Influence in Homogeneous Clayey Soils

Fig. 9 shows the lateral load versus lateral deflection response of the piles in clayey soils. The loads shown here correspond to the symmetric half of the pile section. In this case, it is interesting to note a different trend than that observed in the case of sandy soils. In the presence of vertical load, the lateral load developed at all deflections is less than the corresponding load developed under pure lateral load. The reduction is not significant for vertical loads up to $0.6V_{ult}$. Aubeny et al. (2003) have reported similar findings for piles in clayey soils through finite-element analysis of suction caissons under inclined loads. They have also found that the horizontal anchor load capacity is not significantly affected by verti-

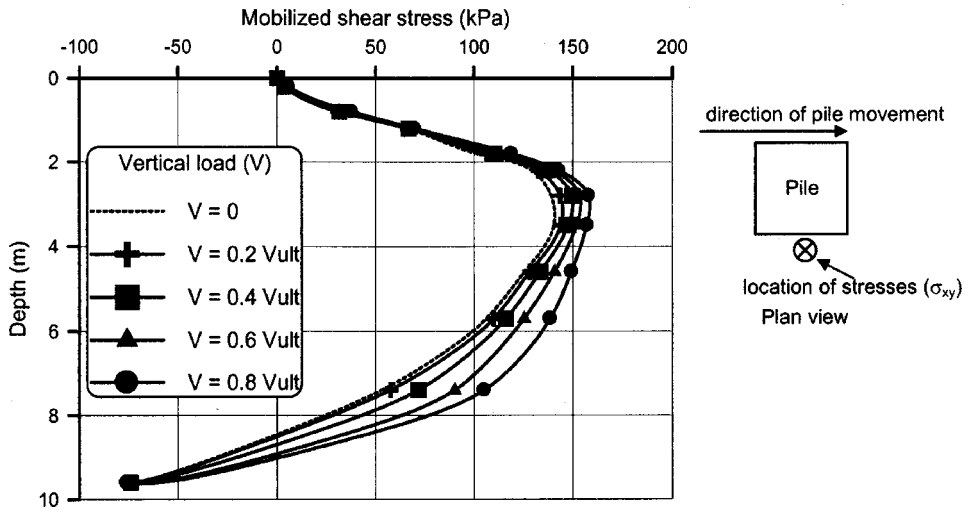

Fig. 7. Variation of shear stress (σ_{xy}) along depth of piles in sand

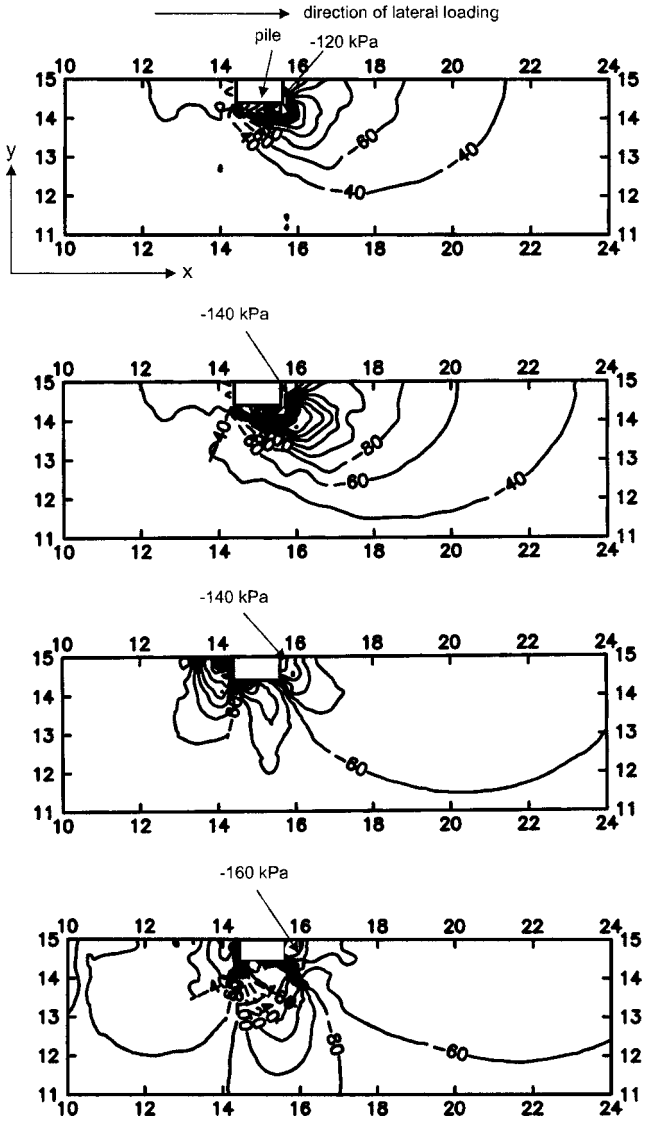

Fig. 8. Lateral and shear stress contours in *xy*-plane at 2.8 m depth from ground surface in sands: (a) σ_{xx} contours for pure lateral loading case; (b) σ_{xx} contours with vertical load of $0.8V_{ult}$; (c) σ_{xy} contours for pure lateral loading; and (d) σ_{xy} contours with vertical load of $0.8V_{ult}$

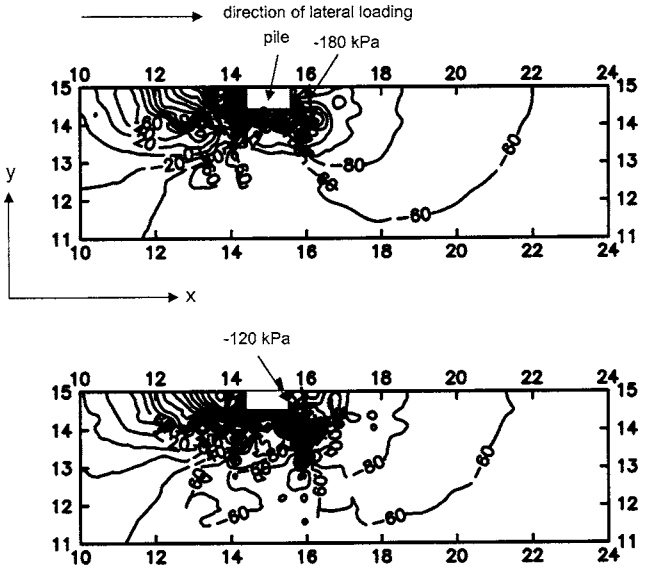

Fig. 10. Lateral stress contours in *xy*-plane at 2.8 m from ground surface in clayey soils: (a) σ_{xx} contours under pure lateral loading; (b) σ_{xx} contours with vertical load of $0.8V_{ult}$

cal components of load for load orientation up to 15°. However, in the present study at a higher vertical load level of $0.8V_{ult}$, the reduction is significant: 20% of the pile capacity. It is clear that the vertical load decreases the lateral load capacity of piles in clayey soils. This reduction in a pile's lateral capacity can be attributed to the early failure of interfaces in the presence of vertical loads. Once the interface between the pile and the surrounding clayey soils fails, further lateral deformation of the pile will not result in increased lateral stresses in the soil around the pile. This reduction in lateral soil stresses is illustrated in Fig. 10, which shows the contours of lateral soil stresses (σ_{xx}) at a lateral deflection of 0.1B and at a depth of 2.8 m from the ground surface for pure lateral loading and with a vertical load of $0.8V_{ult}$. This reduction in lateral soil stresses will lead to development of lower resistance to lateral pile deformation in the presence of vertical load.

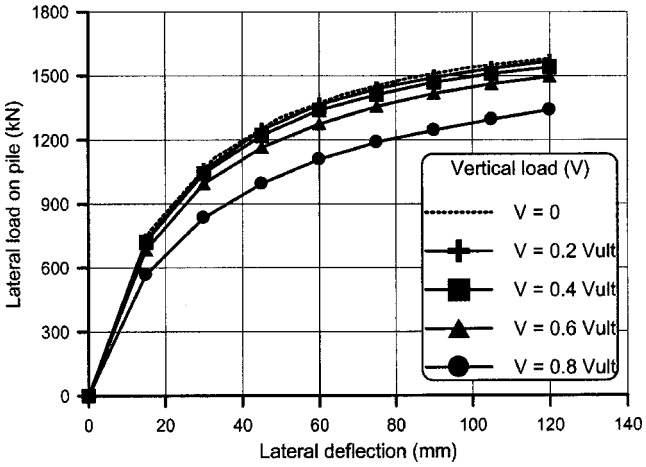

Fig. 9. Lateral load-deflection curves of piles in clayey soils

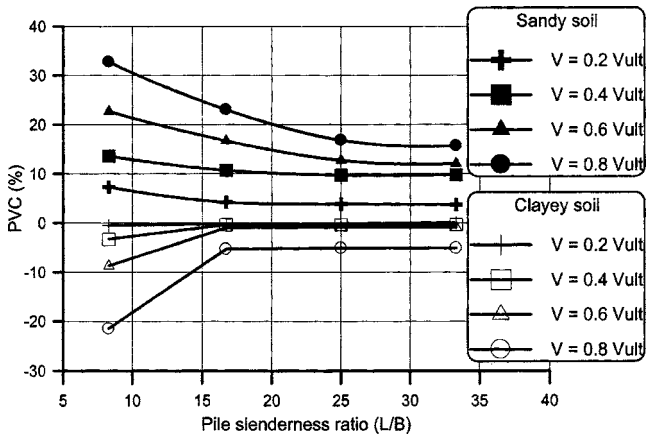

Fig. 11. PVC at various L/B with respect to pile length (L)

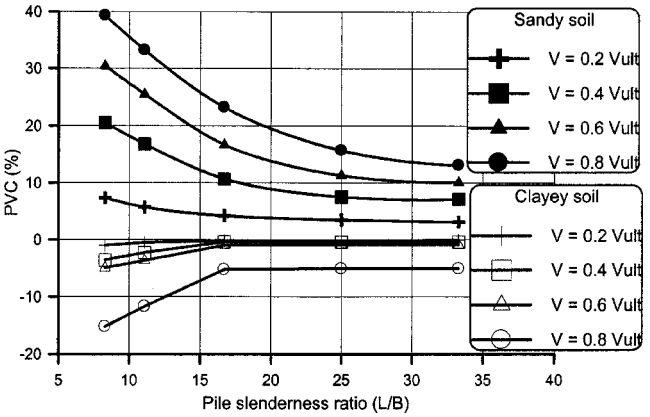

Fig. 12. PVC at various L/B with respect to pile width (B)

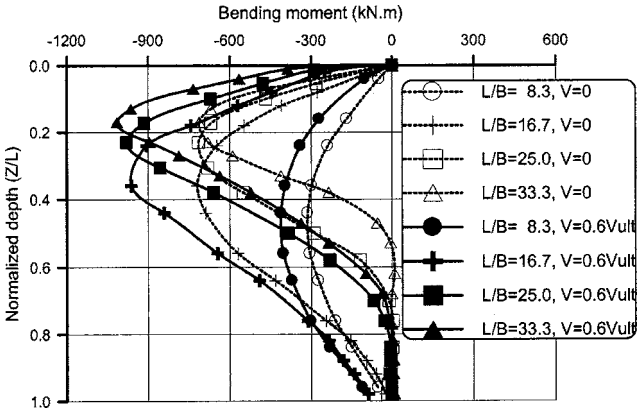

Fig. 14. Bending moments developed in pile section in sandy soils at 0.1B displacement

Influence of the Pile Slenderness Ratio (L/B)

The influence of the pile slenderness ratio (L/B) under combined loading was studied by performing 3D finite-element analysis of a 600 by 600×600 mm square pile with different pile lengths of 5, 10, 15, and 20 m. Similarly, 3D finite-element analyses were also performed by keeping the pile length constant at 10 m and varying the pile widths to 300, 400, 600, 900, and 1,200 mm. All these analyses were performed separately for both clayey soils and sandy soils in the same manner as described earlier.

Based on the numerical results obtained, the PVC with respect to different levels of vertical loads is calculated for various L/B ratios with respect to various pile length (L) and widths (B) considered in the analysis. The PVC is defined as follows in terms of the lateral load capacity with vertical load (LCWV) and the lateral capacity under pure lateral loading (LCPL)

$$\text{PVC} = \frac{\text{LCWV} - \text{LCPL}}{\text{LCPL}} \times 100\% \tag{1}$$

The results have shown that the influence of vertical load decreases with an increase in slenderness ratio of piles at all vertical load levels for both types of soils. In general, it was found that the influence of vertical load with respect to the pile slenderness ratio (L/B) was found to be more in the case of sandy soils than in clayey soils. The influence of the pile slenderness ratio (L/B) on the PVC values observed for both types of soils at a lateral deflection of 0.1B with respect to constant width of pile (B) and varying pile length (L) is shown in Fig. 11. Similar results for a pile with a constant length of 10 m and a varying width B are shown in Fig. 12. It could be observed that the trends are more or less similar in both the cases.

In the case of sandy soils, the presence of a vertical load has increased the lateral load capacity at all slenderness ratios. However, in the case of clayey soils, the influence of vertical load is observed only at the small L/B ratio of 8.3. The PVC values remained more or less constant beyond an L/B ratio of 16.7 in the case of clayey soils. On the other hand, in the case of sandy soils, the PVC values are dependent on both L/B value and the level of vertical load. The PVC value was found to be dependent even up to an L/B value of 33 in the case of sandy soils.

As noted above, the influence of vertical loads keeps decreasing as the L/B ratio increases. This can be directly attributed to the reducing intensity of vertical pressure at larger depths caused by load dispersion effects. In turn this leads to lesser changes in confining stresses at larger depths caused by vertical load applied at the surface. As the soil strength is related to the operating confining stress, the increase in pile capacity can be expected to

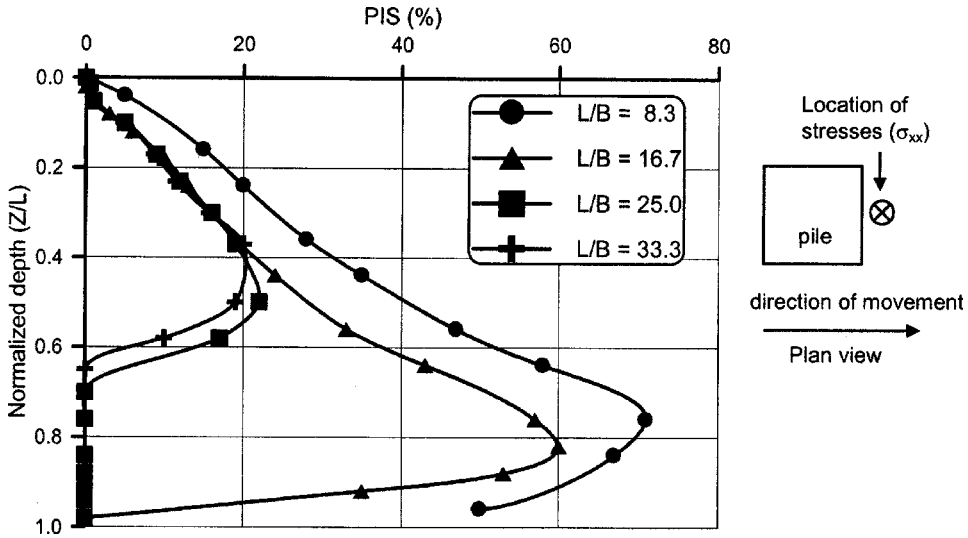

Fig. 13. Percentage increase in lateral soil stresses (PIS) in front of pile at different L/B ratios

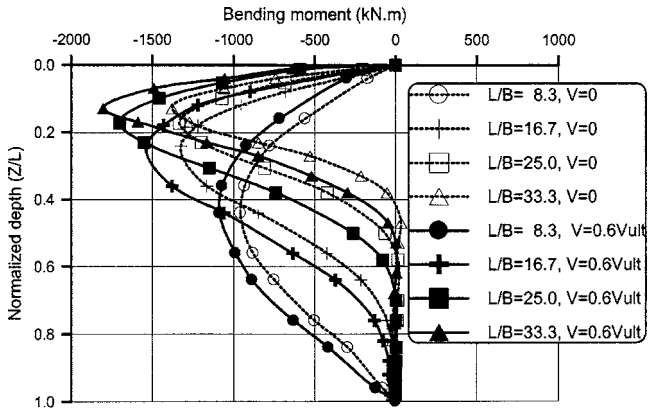

Fig. 15. Bending moments developed in pile section in clayey soils at 0.1B displacement

be lower for longer piles. This aspect is examined through the percentage increase in lateral soil stresses in front of the pile for various L/B ratios. A quantity termed "PIS" is defined as follows as the percentage increase in lateral soil stress (σ_{xx}) in the presence of vertical load (LSWV) as compared to the corresponding lateral soil stress under pure lateral loading (LSPL)

$$\text{PIS} = \frac{\text{LSWV} - \text{LSPL}}{\text{LSPL}} \times 100\% \quad (2)$$

Fig. 13 shows typical PIS values for various L/B ratios at vertical load level of $0.8V_{ult}$ and lateral deflection of 0.1B. The influence of L/B on PIS values can be clearly seen in the figure. The PIS values increased considerably and over longer lengths for shorter piles as compared to longer piles.

For structural design of piles, the bending moments developed in the pile section are important. The influence of combined loading on the bending moments developed in the pile section has been examined from the results obtained. The bending moments developed in the pile section have been estimated using the well known flexural equation from the vertical stresses (σ_{zz}) developed in the pile section. Figs. 14 and 15 show the influence of vertical load on the bending moments developed in the pile section for different L/B ratios and typical vertical load level of $0.6V_{ult}$. Tables 2 and 3 summarize the bending moments developed along the normalized length (Z/L; Z is the depth from ground surface and L is the length of the pile) for different L/B ratios and different vertical load levels for both types of soils. Here, Z_{max} is the depth from the surface at which maximum bending moment occurred and Z_o is the depth at which the bending moment is zero.

From the data presented, the maximum bending moment developed in the pile section is observed to increase with both vertical load levels and L/B ratio. The depth at which the maximum bending moment occurred was influenced very little by the presence of vertical loads in both clayey and sandy soils. In the case of sandy soils, the point of zero bending moment moved down with increasing vertical load levels for long piles ($L/B > 16$). On the other hand, the point of zero bending moment is not much affected by the presence of vertical loads in the case of clayey soils for all lengths of piles. This result shows that even relatively long piles may behave like short piles in the case of sandy soils and when subjected to combined loading. The results have made it clear that the design bending moment in piles is higher under combined loading as compared to the piles under pure lateral loading. The exact increase in the bending moment depends very much on the dimensions and properties of the pile, stiffness and strength properties of the soil, and the level of vertical and lateral loads.

Conclusions

The behavior of single piles subjected to combined vertical and lateral loads has been investigated in the paper through a series of 3D finite-element analyses. Based on the results from these analyses, the following conclusions can be drawn:

1. The response of the piles in both clayey and sandy soils under lateral loads is influenced by the presence of vertical loads.
2. The presence of vertical loads increases the lateral load ca-

Table 2. Bending Moments in Pile Section in Sandy Soils at Lateral Displacement of 0.1B

L/B	Vertical load in terms of V_{ult}	Lateral load H (kN)	Maximum BM M_{max} (kN m)	Normalized BM $M_{max}/(HL)$	Z_{max}/L	Z_o/L
8.3	0	110	313	0.57	0.44	1.0
	0.2	118	343	0.58	0.44	1.0
	0.4	128	378	0.59	0.44	1.0
	0.6	137	412	0.60	0.44	1.0
16.7	0	178	720	0.40	0.36	1.0
	0.2	185	787	0.42	0.36	1.0
	0.4	191	846	0.44	0.36	1.0
	0.6	198	962	0.48	0.36	1.0
25.0	0	184	723	0.26	0.25	0.70
	0.2	192	790	0.27	0.22	0.92
	0.4	200	850	0.28	0.22	0.98
	0.6	214	980	0.30	0.22	1.0
33.3	0	185	725	0.20	0.18	0.56
	0.2	193	848	0.22	0.17	0.67
	0.4	201	981	0.24	0.17	0.76
	0.6	215	1030	0.24	0.17	0.90

Table 3. Bending Moments in Pile Section in Clayey Soils at Lateral Displacement of 0.1B

L/B	Vertical load in terms of V_{ult}	Lateral load H (kN)	Maximum BM M_{max} (kN m)	Normalized BM $M_{max}/(HL)$	Z_{max}/L	Z_o/L
8.3	0	450	958	0.43	0.45	1.0
	0.2	446	1003	0.45	0.45	1.0
	0.4	435	1042	0.48	0.45	1.0
	0.6	405	1088	0.54	0.45	1.0
16.7	0	529	1325	0.25	0.25	0.87
	0.2	529	1402	0.26	0.25	0.88
	0.4	528	1486	0.28	0.25	0.90
	0.6	525	1537	0.30	0.25	0.93
25.0	0	530	1335	0.17	0.17	0.58
	0.2	529	1465	0.18	0.17	0.59
	0.4	528	1587	0.20	0.17	0.61
	0.6	525	1700	0.22	0.17	0.63
33.3	0	530	1372	0.13	0.13	0.44
	0.2	529	1470	0.14	0.13	0.45
	0.4	528	1630	0.15	0.13	0.48
	0.6	526	1802	0.17	0.13	0.51

pacity of piles in sandy soils by as much as 40% depending on the level of vertical load.

3. The presence of a vertical load marginally reduces the lateral capacity of piles in clayey soils for vertical load levels up to $0.6V_{ult}$ and by as much as 20% for higher vertical load levels.
4. The lateral response of piles under combined loading is also dependent on the L/B ratio of the pile. As the L/B ratio increases, the influence of vertical load on the lateral capacity reduces. The influence of vertical loads remains constant beyond an L/B ratio of 25 in sandy soils and 16 in clayey soils.
5. The design bending moment in the pile section is influenced by the presence of vertical loads. The maximum bending moment increases by as much as 30 to 35% in sandy soils for the range of pile dimensions and soil properties examined in this paper. In the case of clayey soils, the maximum bending moment increases by about 10 to 15% for L/B values less than 15 and about 30% for longer piles.

Acknowledgments

The writers would like to thank the director, CBRI, for encouragement and interest in this research. The first writer is also thankful to the director, CBRI, for the leave sanctioned to pursue his doctoral research as an external PhD scholar at IIT, Madras, Chennai.

References

Anagnostopoulos, C., and Georgiadis, M. (1993). "Interaction of axial and lateral pile responses." *J. Geotech. Engrg.*, 119(4), 793–798.

Aubeny, C. P., Han, S. W., and Murff, J. D. (2003). "Inclined load capacity of suction caissons." *Int. J. Numer. Analyt. Meth. Geomech.*, 27, 1235–1254.

Banerjee, P. K., and Davis, T. G. (1978). "The behaviour of axially and laterally loaded single piles embedded in non-homogeneous soils." *Geotechnique*, 28(3), 309–326.

Bartolomey, A. A. (1977). "Experimental analysis of pile groups under lateral loads." *Proc., Special Session 10 of the 9th Int. Conf. on Soil Mech. and Found. Engrg.*, 187–188.

Bowles, J. E. (1988). *Foundation analysis and design*, 4th Ed., McGraw-Hill, New York.

Broms, B. B. (1964). "Lateral resistance of piles in cohesionless soils." *J. Soil Mech. and Found. Div.*, 90(3), 123–156.

Brown, D. A., and Shie, C. F. (1991). "Some numerical experiments with a three-dimensional finite element model of a laterally loaded pile." *Comp. Geotechn.*, 12, 149–162.

Coyle, H. M., and Reese, L. C. (1966). "Load transfer for axially loaded piles in clay." *J. Soil Mech. and Found. Div.*, 92(2), 1–26.

Davisson, M. T., and Robinson, K. E. (1965). "Bending and buckling of partially embedded piles." *Proc., 6th Int. Conf. on Soil Mech. and Found. Engrg.*, Montreal, 243–246.

Desai, C. S. (1974). "Numerical design-analysis for piles in sands." *J. Geotech. Engrg. Div.*, 100(6), 613–635.

Goryunov, B. F. (1975). "Discussion on analysis of piles subjected to the combined action of vertical and horizontal loads." *J. Soil Mech. Found. Eng.*, 10(1), 10.

Jain, N. K., Ranjan, G., and Ramasamy, G. (1987). "Effect of vertical load on flexural behaviour of piles." *J. Geotech. Engrg.*, 18, 185–204.

Kimura, M., Adachi, T., Kamei, H., and Zhang, F. (1995). "3-D finite element analyses of the ultimate behaviour of laterally loaded cast-in-place concrete piles." *Proc., 5th Int. Symp. on Numerical Models in Geomechanics*, G. N. Pande and S. Pietruszczak, eds., NUMOG V.A.A. Balkema, Rotterdam, 589–594.

Kraft Jr., L. M., Ray, R. P., and Kagawa, T. (1981). "Theoretical t-z curves." *J. Geotech. Engrg. Div.*, 107(11), 1543–1562.

Matlock, H., and Reese, L. C. (1960). "Generalized solutions for laterally loaded piles." *J. Soil Mech. and Found. Div.*, 86(SM5), 63–89.

McNulty, J. F. (1956). "Thrust loading on piles." *J. Soil Mech. and Found. Div.*, 82(SM2), 1–25.

Muqtadir, A., and Desai, C. S. (1986). "Three-dimensional analysis of a pile group foundation." *Int. J. Numer. Analyt. Meth. Geomech.*, 39(1), 97–111.

Nayak, G. C., and Zienkiewicz, O. C. (1972). "Elasto-plastic stress analysis: generalisation for various constitutive relations including strain softening." *Int. J. Numer. Methods Eng.*, 5, 113–135.

Pise, P. J. (1975). "Investigation on laterally loaded pile groups." *Symp. on Recent Developments in the Analysis of Soil Behaviour and its Application to Geotechnical Structures*, Univ. of New South Wales,

Australia, 129–144.
Poulos, H. G. (1968). "Analysis of the settlement of pile groups." *Geotechnique*, 18(4), 449–471.
Poulos, H. G. (1971). "Behaviour of laterally loaded piles: I—single piles." *J. Soil Mech. and Found. Div.*, 97(5), 711–731.
Poulos, H. G., and Davis, E. H. (1980). "Pile foundation analysis and design." Wiley, New York.
Ramasamy, G. (1974). "Flexural behaviour of axially and laterally loaded individual piles and group of piles." Ph.D. thesis, Indian Institute of Science, Bangalore, India.
Reese, L. C., Cox, W. R., and Koop, F. D. (1974). "Analysis of laterally loaded pile in sand." *Proc. 6th Annual Offshore Technology Conf.*, Houston, 2080.
Sarochan, E. A., and Bykov, V. I. (1976). "Performance of groups of cast in place piles subjected to horizontal loading." *J. Soil Mech. Found. Eng.*, 13(3), 157–161.
Trochanis, A. M., Bielak, J., and Christiano, P. (1991). "Three-dimensional nonlinear study of piles." *J. Geotech. Engrg.*, 117(3), 429–447.
Wang, G., and Sitar, N. (2004). "Numerical analysis of piles in elasto-plastic soils under axial loading." *Proc., 17th ASCE Eng. Mech. Conf.*, Univ. of Delaware, 1–8.
Xu, K. J., and Poulos, H. G. (2000). "General elastic analysis of piles and pile groups." *Int. J. Numer. Analyt. Meth. Geomech.*, 24, 1109–1138.
Yang, Z., and Jeremic, B. (2002). "Numerical analysis of pile behaviour under lateral loads in layered elastic-plastic soils." *Int. J. Numer. Analyt. Meth. Geomech.*, 26, 1385–1406.
Yang, Z., and Jeremic, B. (2005). "Study of soil layering effects on lateral loading behaviour of piles." *J. Geotech. Geoenviron. Eng.*, 131(6), 762–770.
Zhu, H., and Chang, M. F. (2002). "Load transfer curves along bored piles considering modulus degradation." *J. Geotech. Geoenviron. Eng.*, 128(9), 764–774.
Zhukov, N. V., and Balov, I. L. (1978). "Investigation of the effect of a vertical surcharge of horizontal displacements and resistance of pile columns to horizontal loads." *J. Soil Mech. Found. Eng.*, 15(1), 16–21.